# Reduction of electronic delay in active noise control systems—A multirate signal processing approach

Mingsian R. Bai,[a] Yuanpei Lin, and Jienwen Lai
*Department of Mechanical Engineering, National Chiao-Tung University, 1001 Ta-Hsueh Road, Hsin-Chu 300, Taiwan, Republic of China*

(Received 30 November 2000; accepted for publication 5 November 2001)

Electronic delay has been a critical problem in active noise control (ANC) systems. This is true whether a feedforward structure or a feedback structure is adopted. In particular, excessive delays would create a causality problem in a feedforward ANC system of a finite-length duct. This paper suggests a multirate signal-processing approach for minimizing the electronic delay in the control loop. In this approach, digital controllers are required in decimation and interpolation of discrete-time signals. The computation efficiency is further enhanced by a polyphase method, where the phases of low-pass finite impulse response (FIR) filters must be carefully designed to avoid unnecessary delays. Frequency domain optimization procedures based on $H_1$, $H_2$, and $H_\infty$ norms, respectively, are utilized in the FIR filter design. The proposed method was implemented by using a floating-point digital signal processor. Experimental results showed that the multirate approach remains effective for suppressing a broadband (200–600 Hz) noise in a duct with a minimum upstream measurement microphone placement of 20 cm.  [DOI: 10.1121/1.1432980]

PACS numbers: 43.50.Ki [MRS]

## NOMENCLATURE

| | |
|---|---|
| $p_{sp}$ | equivalent primary pressure source |
| $p_{sa}$ | equivalent secondary pressure source |
| $Z_{sp}$ | equivalent primary source impedance |
| $Z_{sa}$ | equivalent secondary source impedance |
| $Z_0$ | radiation impedance at the duct opening |
| $C(z)$ | digital filter of active controller |
| $H_{\mathrm{d}}(e^{j\omega})$ | frequency response template |
| $Bl$ | electromagnetic transduction constant |
| $z_{\mathrm{M}}$ | mechanical mobility of loudspeaker |
| $u_{\mathrm{c}}, f_{\mathrm{c}}$ | cone velocity and force |

## I. INTRODUCTION

Active control for noise in ducts has been investigated by researchers in the area of active noise control (ANC) for decades.[1–4] A great majority of ANC systems to date has been realized by digital systems.[4] Although digital systems provide many advantages over the analog counterpart, they suffer from several design constraints. In particular, the electronic delay during analog-to-digital (AD) conversion and digital-to-analog (DA) conversion, low-pass antialiasing and reconstruction (or smoothing) filtering has been a critical problem in active noise control systems. These delays along with other inherent delays resulting from computation and transducer dynamics might pose design constraints on ANC systems, which could become quite severe when the application of interest has strict space limitation, e.g., active mufflers for motorcycles. These design constraints apply to both feedback control and feedforward control. Specifically, excessive delays would limit the achievable performance and stability margin in a feedback ANC system.[5] Causality is usually not a problem for periodic signals so long as the controller has a long enough impulse response to produce the properly phased cancellation filter. In conventional signal-processing applications, delay is usually not an important issue. Pure delay is usually tolerated because the waveform is preserved. However, delay becomes crucial in control systems, especially for ANC applications that generally involve relatively large bandwidth. Excessive delays could create causality problems in a feedforward ANC system of a finite length duct if the noise of concern is broadband and random in nature. Causality constraint refers to the condition under which the delay in the acoustical path is greater than the electronic path such that the resulting controller is causal and hence implementable. Under the causality constraint, delays in low sampling rate systems generally result in impractical requirement on physical dimension.[1,4]

To combat the delay problem in the control loop, this paper proposes a digital signal-processing scheme based on the multirate concept that is a fast growing area in many applications.[6,7] In this approach, digital controllers are required in decimation and interpolation of discrete-time signals. To enhance computation efficiency, a polyphase method is employed in filter design.[8–10] In the multirate ANC system, a factor of 8 was used for upsampling and downsampling. This resampling process raises the nominal sampling frequency of controller 2 kHz to 16 kHz during AD/DA conversion, which significantly reduces the sample delays. As a crucial part in the polyphase design, the phases of low-pass finite impulse response (FIR) filters must be carefully designed to avoid unnecessary delays. To this end, optimization

[a]Electronic mail: msbai@cc.nctu.edu.tw

 

procedures in frequency domain based on $H_1$, $H_2$, and $H_\infty$ norms, respectively, are utilized in the design.[11–13]

One fundamental question may be naturally raised: why not simply run the ANC system at a very high sampling rate? Delay would then be low, and there would be no need for the multirate filters at all. Unfortunately, there are several subtle points that may prohibit the use of this seemingly straightforward approach. First, the effective control bandwidth for the physical system would only be in a small portion of the total frequency span. This causes an ill-conditioned eigenvalue spread and poor frequency resolution. Second, numerical problems may arise so that a filter with lightly damped poles may easily become unstable. Third, impractically long taps may be needed to implement a FIR filter for very high sampling rate operation, and the computations may not be completed within one sample. Therefore, we chose to take the indirect approach, multirate signal processing. It was also pointed out by the reviewer that the idea of using multirate, or oversampling, has been applied to ANC by Brammer *et al.* for headsets.[14] In their work, a digital ANC headset based on adaptive feedforward control has been developed, and the performance measured on human subjects using helicopter noise reproduced in a reverberation room. Their system demonstrated more than 10-dB noise reduction at frequencies 16 to 250 Hz. A dual-rate sampling structure is used. The signals at the reference and error microphones were oversampled, and the control signal computation and updating were performed at a decimated rate. This technique reduces the delay in the control path by increasing the sampling frequency of AD and DA converters and, at the same time, permits the low-frequency performance of the FIR filter to be improved. This paper is based on the same motivation, but different from the work of Brammer *et al.* in the following aspects. First, the nature of the problem in this paper is quite different from the headset problem. The problem investigated in this paper is a one-dimensional duct problem where the complexity of its plant dynamics is much higher than the zero-dimensional headset problem. Second, the ANC structure examined in this paper is the spatially feedforward structure with strong acoustic feedback (from the actuator to the upstream sensor). Acoustic feedback creates a undesirable positive feedback and may destabilize the system, which calls for different controller design than the headset problem. In headset problems, acoustic feedback is virtually negligible and conventional filtered-X LMS is sufficient. On the other hand, the significance of delay to the spatially feedforward system is examined in the paper. How to reduce delay becomes a critical issue due to the causality constraint imposed by the feasible physical dimension. Third, in the paper details of how one would implement the multirate scheme are presented, and the effectiveness of the approach with regard to physical dimension is quantitatively evaluated. As pointed out by Brammer *et al.*, electronic delay can be reduced by running IO operations at a high sampling rate, while performing computation at a low sampling rate. However, cautions must be taken to implement this idea properly. Two digital low-pass filters are needed to eliminate the artifacts in the decimation and interpolation processes. Without these protection measures, one might get erroneous results from the up/down sampling. Unlike typical multirate signal processing, however, these low-pass filters entail special design in the context of active control, where delay within the control bandwidth has profound effects on performance and stability. Another key step regarding implementation is the enhancement of computational efficiency by polyphase filters. As compared to the primitive up/down sampling scheme, where idling of CPU power arises due to redundancies such as dropping of data during decimation and convolution with zero during interpolation, great saving of computations can be obtained by reformulating the filters by polyphase structures. These implementation techniques are not trivial but extremely important to a properly functioning multirate system. Without handling these crucial steps correctly, the system may result in poor efficiency and even failure of performance.

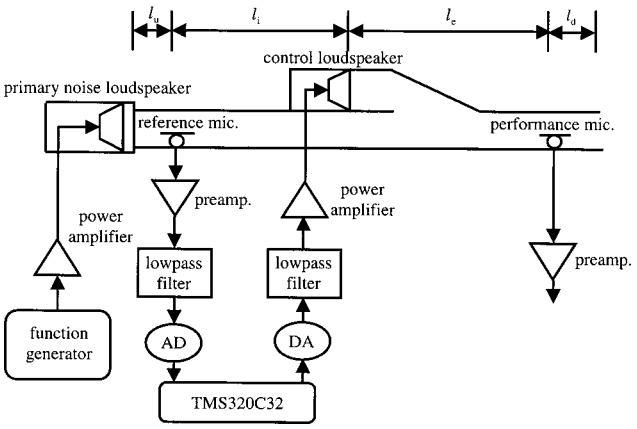


FIG. 1. The spatially feedforward structure of ANC system.

The proposed method was implemented by using a floating-point digital signal processor (DSP). Experimental results indicated that the multirate approach is effective for suppressing broadband noise in a spatially feedforward duct ANC system. Some technical considerations involved in implementation will also be addressed in the paper.

## II. EFFECTS OF DELAY ON A SPATIALLY FEEDFORWARD SYSTEM

The ANC system chosen for investigation in this work is the *spatially feedforward structure*[15] for ducts, which has been a prevailing ANC structure in that it can be used when a nonacoustical reference is unavailable and broadband attenuation is desired. In what follows, only key results relevant to the discussion are presented and detailed derivations can be found in the literature[16] and are thus omitted for brevity.

Figure 1(a) depicts a duct ANC system with spatially feedforward structure. In this structure, an upstream microphone is employed to measure the sound field near the primary noise source. The signal from the upstream microphone is fed to the controller, which produces a control signal to drive a downstream control speaker that generates an antifield to interact with the primary noise field. The goal of active control is to minimize the residual noise downstream of the control speaker. The definitions of symbols can be found in the Nomenclature and Ref. 15.

TABLE I. The electro-mechanical parameters of a moving-coil speaker.

| Electro-mechanical constants | |
|---|---|
| $M_M$ | 13.83 g |
| $R_M$ | 1.3 ohms |
| $C_M$ | 874 $\mu$m/N |
| $R$ | 6.88 ohms |
| $L$ | 0.68 mH |
| $Bl$ | 4.85 T-m |

Munjal and Eriksson[16] derived the ideal controller capable of achieving global noise cancellation downstream of the control source in a finite-length duct

$$C=-\frac{Z_{sa}}{Y_0}\left(\frac{e^{-jkl_i}}{1-e^{-2jkl_i}}\right)=C_0\cdot C_r, \tag{1}$$

where $Z_{sa}$ is the equivalent acoustic impedance of the control source, $Y_0=c/S$ is the characteristic impedance of the duct, $c$ is the sound speed, $S$ is the cross-sectional area of the duct, $k$ is the wave number, and $l_i$ is the distance between the upstream measurement microphone and the control source. In Eq. (1), $C_0\equiv -Z_{sa}/Y_0$ is a function of the finite impedance $Z_{sa}$, which depends only on the electro-mechanical parameters of the control source. On the other hand, $C_r \equiv e^{-jkl_i}/1-e^{-2jkl_i}$ takes the form of the so-called *repetitive controller*.[17] Due to the infinite number of poles on the imaginary axis, both frequency response and impulse response of the ideal controller exhibit patterns of comb-typed periodic peaks ($\Delta f=c/2l_i, \Delta t=2l_i/c$). The fundamental reason for the repetitiveness is essentially rooted in the acoustic feedback.

In the course of analysis, we shall develop some physical insights into the causality of the ANC system by examining the aforementioned ideal controller. It is observed from Eq. (1) that the implementation of the ideal controller requires the knowledge of the control source impedance $Z_{sa}$. In what follows, $Z_{sa}$ will be expressed explicitly in terms of the electro-mechanical parameters of speaker. Detailed analysis will show that $Z_{sa}$ can be expressed as[15]

$$Z_{sa}=\frac{1}{\rho S^2}\left(\frac{1}{z_M}+\frac{B^2l^2}{R+j\Omega L}\right), \tag{2}$$

where $R$ is the total equivalent resistance of the coil, $L$ is the equivalent inductance of the coil, $Bl$ is the coil constant, $z_M$ is the mechanical mobility, and $\Omega$ is the analog frequency in rad/s. In the expression of Eq. (2), $Z_{sa}$ depends solely on the speaker parameters $R$, $L$, and $Bl$ that can be identified in advance.[18] In the experimental setup in our case, these parameters were identified and listed in Table I. With the transducer dynamics taken into account, it has been shown in Ref. 15 that the resulting controller is

$$C'=-\frac{1}{G_{XDCR}}\left(\frac{e^{-jkl_i}}{1-e^{-2jkl_i}}\right), \tag{3}$$

where

$$G_{XDCR}=(g_p g_m G_s)\frac{Y_0}{Z_{sa}} \tag{4}$$

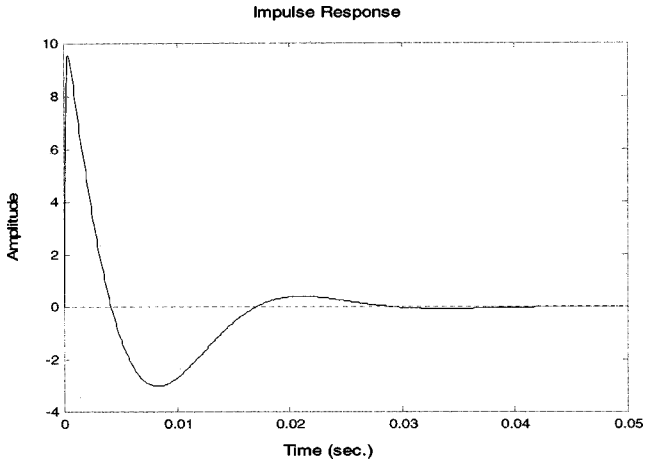


FIG. 2. The impulse response of transducer dynamics $G_{XDCR}$.

represents the overall transducer dynamics, where $g_p$ and $g_m$ denote the constant gains of the power amplifier and the microphone, respectively, and $G_s$ is the frequency response function of the speaker

$$G_s=\frac{Bl}{S(R+j\Omega L)}. \tag{5}$$

Inspection of Eq. (3) reveals that the transducer response must compete with the propagation delay $e^{-jkl_i}$ in the acoustic path. More precisely, the condition under which the resulting controller is causal is that the term $e^{-jkl_i}/G_{XDCR}$ must be causal. This is an important causality constraint one must observe, particularly for the spatially feedforward structure.

Omitting the constants $g_p$, $g_m$, and $Y_0$ in Eq. (4), $G_{XDCR}$ can be written as a third-order system

$$\begin{aligned} G_{XDCR}\sim (BlR_MC_Ms)/[&M_MR_MC_MLs^3 \\ &+(C_ML+M_MR_MC_MR)s^2 \\ &+(C_MR+R_ML+B^2l^2R_MC_M)s+R_MR], \end{aligned} \tag{6}$$

where $M_M$, $R_M$, $C_M$ are mechanical mass, viscous damping, and mechanical compliance, respectively. For example, we can use the data in Table I and plot the impulse response of $G_{XDCR}$, as shown in Fig. 2. The first peak is at 0.3 ms, which amounts to 0.6 delay samples at 2-kHz sampling rate. Using this as a criterion of transducer delay, the length of the duct must be greater than 343 m/s (at 20 °C) $\times 0.3$ ms $=0.103$ m to meet the causality condition.

In addition to transducer delay, other types of electronic delay include all possible delays in the antialiasing/smoothing filters (denoted as $\delta_F$), AD/DA conversion, and the one-sample processing time (provided computations are completed within one sample), where the last two terms can be lumped into a single term $\delta_T$. These delays, together with the group delays of transducer and the digital controller (denoted as $\delta_X$ and $\delta_W$, respectively), constitute the total electronic delay

$$\delta_E=\delta_X+\delta_F+\delta_T+\delta_W. \tag{7}$$

The electronic delays are summarized in Fig. 3. The transducer delay $\delta_X$ is estimated according to the first peak of the impulse response of Eq. (6). The analog filter delay can be

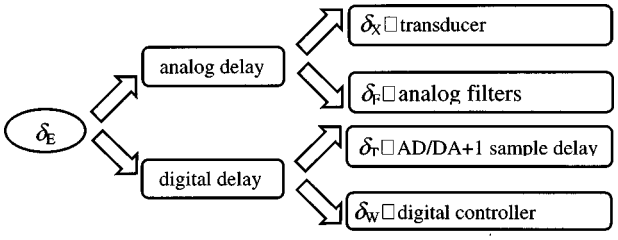


FIG. 3. The elements of electronic delay $\delta_E$.

estimated by $\delta_F = n/8f_c$, where $n$ is the filter order and $f_c$ is the cutoff frequency.[19] The one-sample delay and the AD/DA delay together can be estimated by $\delta_T = \Delta\Phi/360\Delta f$, where $\Phi$ is the unwrapped phase (in degrees) of the DSP frequency response in "echo" operation.

A formal statement of the causality constraint on the spatially feedforward ANC system can now be written as

$$\delta_A \geq \delta_E, \tag{8}$$

where the acoustical delay $\delta_A = l_i/c$, $l_i$ being the distance between the upstream microphone and the control speaker. Violation of the causality constraint, i.e., the electronic delay is greater than the acoustical delay, will result in a noncausal controller. An optimal causal approximation to a noncausal controller may well exist theoretically and converge to the Wiener filter solution.[20] However, in practice, violation of causality would give rise to performance degradation of an ANC system, depending on the degree of violation. For the compensators to be implementable, the acausal part must be truncated to construct FIR filters. Physically, the causality constraint sets the minimum length of duct for which random noise can be effectively canceled

$$(l_i)_{\min} \geq c\,\delta_E. \tag{9}$$

Therefore, a system with large electronic delay will generally lead to impractical length of duct, especially when the sampling rate is low. For example, the sampling rate is selected to be 2 kHz in our experiment, rendering an estimated electronic delay of 4.3 samples. This corresponds to a minimal duct length of 73 cm. From the delay components listed in Table II, it can be observed that $\delta_F$ and $\delta_T$ contribute most significantly to the overall delay. Given a length limitation of a duct, one must strive to minimize the electronic delay in order to meet the causality constraint. To this end, a multirate signal-processing technique is developed in this work for reducing the delays $\delta_F$ and $\delta_T$.

TABLE II. The elements of electronic delay measured in samples (on a 2-kHz basis).

| Delay elements | Conventional implementation (samples) | Multirate implementation (samples) |
|---|---|---|
| $\delta_X$ | 0.6 | 0.6 |
| $\delta_F$ | 2.2 | 0.3[a] |
| $\delta_T$ | 1.5 | 0.7 |
| Total delay | 4.3 | 1.6 |

[a]Includes the delay of digital LPF = 0.1 samples.

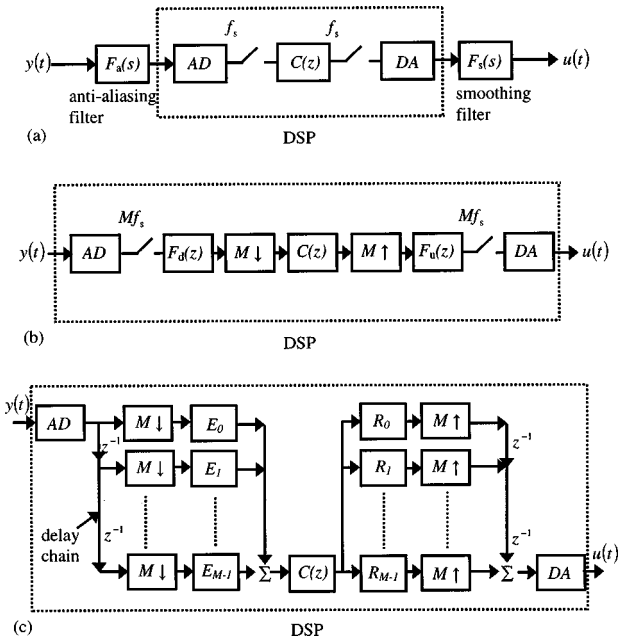


FIG. 4. The structures of implementation for a duct ANC system. (a) The conventional structure; (b) the original multirate structure; (c) the multirate structure using polyphase representation.

## III. MULTIRATE SIGNAL PROCESSING BY POLYPHASE FILTERS

To reduce electronic delay, this paper proposes a digital signal-processing scheme based on the multirate concept. In this approach, only inexpensive analog filters with high cutoff frequency, e.g., 8 kHz, are required. To enhance computation efficiency, a polyphase method is employed in filter design. This technique reduces the delay in the control loop by increasing the sampling frequency of AD and DA converters and, at the same time, permits the low-frequency performance of the FIR filter to be improved.

The block diagram of a conventional ANC system is depicted in Fig. 4(a). The system generally suffers from excessive electronic delay, especially for low sampling rate and/or low filter cutoff frequencies. It may create a causality problem in the ANC system, particularly for the control of broadband random noise where upstream microphone spacing is limited, such as short ducts. It is then highly desirable to minimize, whenever possible, the group delay in the electronic path. To this end, an ANC system based on multirate digital signal processing is developed in the work. The general idea of the multirate ANC system is depicted in Fig. 4(b). In the new structure, the sampling rate of AD and DA converters is raised to a much higher rate, say, $M f_s$, with $M$ being the decimation factor. The continuous-time signal $y(t)$ from the sensor is discretized by an AD converter at a high sampling rate, filtered by a low-pass digital filter, and decimated by a downsampler. The signal is then processed by a low sampling rate ($f_s$) digital controller $C(z)$ to produce an output signal that is in turn interpolated by an expander to the high sampling rate, $M f_s$. In this paper, a fixed controller $C(z)$ is synthesized for the spatially feedforward duct problem. The frequency response samples of the controller are calculated by using Eq. (3). Then, the discrete-time transfer

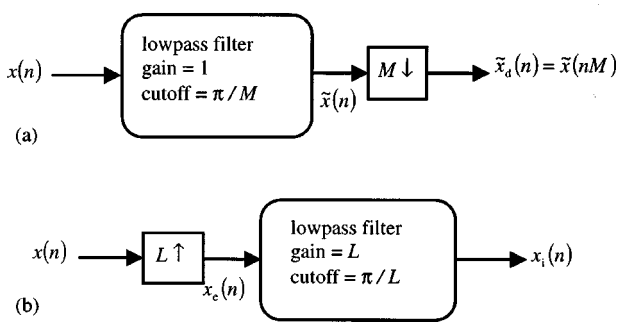


FIG. 5. The decimator and the interpolator. (a) Decimator for sampling rate reduced by a factor $M$; (b) interpolator for sampling rate increased by a factor $L$.

function of the controller $C(z)$ is obtained simply by curve-fitting the frequency response samples, using the MATLAB command *invfreqz*. The details of implementation can be found in Ref. 15. The upsampled signal is low-pass filtered before DA conversion into the continuous-time actuating signal $u(t)$. It is noted that, in this multirate scheme, hardware complexity and the associated delay are reduced because low-pass filtering is all done by software and analog low-pass filters are no longer needed. Efficient implementation of the interpolation and decimation filters forms the basis of a delay-reduced ANC system. Optimization methods can be utilized to calculate the filter coefficients, as will be detailed in the next section. In addition to the reduction of hardware complexity, the AD/DA delay and the one-sample computation delay are almost negligible because the critical processes are operated at a much higher sampling rate, hence the saving of $\delta_T$ and $\delta_F$.

As a final touch, computation efficiency of the multirate ANC system can be drastically enhanced by polyphase filters, as shown in Fig. 4(c), where the decimation factor $M$ and the interpolation factor $L$ are identical. Note that the decimation filter and the interpolation filter both contain delay chains that function essentially as rotating switches.[7]

## IV. FILTER DESIGN BY FREQUENCY-DOMAIN OPTIMIZATION

The decimation and interpolation processes in the foregoing multirate ANC system involve the design of two digital low-pass filters. In order to avoid aliasing in downsampling by a factor of $M$, a low-pass filter is required with a cutoff frequency

$$\omega_N < \pi/M, \tag{10}$$

as illustrated in Fig. 5(a). If the discrete-time input $x(n)$ is filtered by such a filter, then the output $\tilde{x}(n)$ can be downsampled without aliasing. Such a system is called a decimator. On the other hand, to reconstruct the sequence by upsampling with a factor of $L$ requires another low-pass filter with cutoff frequency $\pi/L$ and gain $L$, as shown in Fig. 5(b). Such a system is called an interpolator. In general, FIR filters are employed as the low-pass filters due to the fact that they are inherently stable.

To further improve the computation efficiency, optimization techniques[11] in frequency domain are developed for minimizing the filter length. In terms of $H_1$, $H_2$, and $H_\infty$ norms, the optimization problem of the filter design can be written as follows:[12]

$$\min_{h(k)\in R} \left\| \sum_{k=0}^{K-1} h(k)e^{-j\omega k} - H_d(e^{j\omega}) \right\|_{1,2,\infty}, \tag{11}$$

where $\|\ \|$ denotes the norm, $\omega$ is the digital frequency, $K$ is the tap length of the FIR filter, $h(k)$ is the impulse response (or the filter coefficients) of the FIR filter, and $H_d(e^{j\omega})$ is a low-pass frequency response template. The objective here is to find the filter coefficients $h(k)$ such that the "difference" (measured by 1, 2, or $\infty$ norm) between the desired and the resulting frequency responses is minimized. Globally optimal solutions exist for these problems because they all fall into the class of convex problems.[12,13]

The optimization problem of Eq. (11) can now be solved numerically by subroutines *fminu* (1 norm and 2 norm) and *minimax* ($\infty$ norm) in the MATLAB optimization toolbox.[13] Among these, the $H_2$ optimization problem can also be solved via the least-square method. Express the desired frequency response into a FIR form

$$H_d(z) = \sum_{k=0}^{K-1} h(k)z^{-k}. \tag{12}$$

Substituting the frequency samples $z = e^{j\omega_n}$, $n = 1,2,...,N$, in Eq. (12) leads to the following linear system of equations:

$$\begin{bmatrix} H_d(e^{i\omega_1}) \\ H_d(e^{i\omega_2}) \\ \vdots \\ H_d(e^{i\omega_N}) \end{bmatrix} = \begin{bmatrix} e^{-j\omega_1\times 0} & e^{-j\omega_1\times 1} & \cdots & e^{-j\omega_1\times(K-1)} \\ e^{-j\omega_2\times 0} & \ddots & & e^{-j\omega_2\times(K-1)} \\ \vdots & & \ddots & \vdots \\ e^{-j\omega_N\times 0} & e^{-j\omega_N\times 1} & \cdots & e^{-j\omega_N\times(K-1)} \end{bmatrix} \times \begin{bmatrix} H(0) \\ h(1) \\ \vdots \\ h(K-1) \end{bmatrix}. \tag{13}$$

In matrix notation, Eq. (13) can be written in a more compact form

$$\mathbf{b} = \mathbf{A}\mathbf{x}. \tag{14}$$

The least-square solution of Eq. (14), corresponding to the $H_2$ optimization of Eq. (11), simply reads

$$\mathbf{x} = \mathbf{A}^+\mathbf{b}, \tag{15}$$

where $\mathbf{A}^+ = (\mathbf{A}^H\mathbf{A})^{-1}$, $\mathbf{A}^H\mathbf{b}$ being the *pseudoinverse*[21] of $\mathbf{A}$.

To end this section, an important point regarding how to choose the desired filter response for multirate implementation needs to be addressed. A common practice in multirate signal processing is to employ low-pass filters with linear phase property, where waveform distortion is the only concern. Unfortunately, such an approach did not work for our ANC application because of the undesired group delay intro-

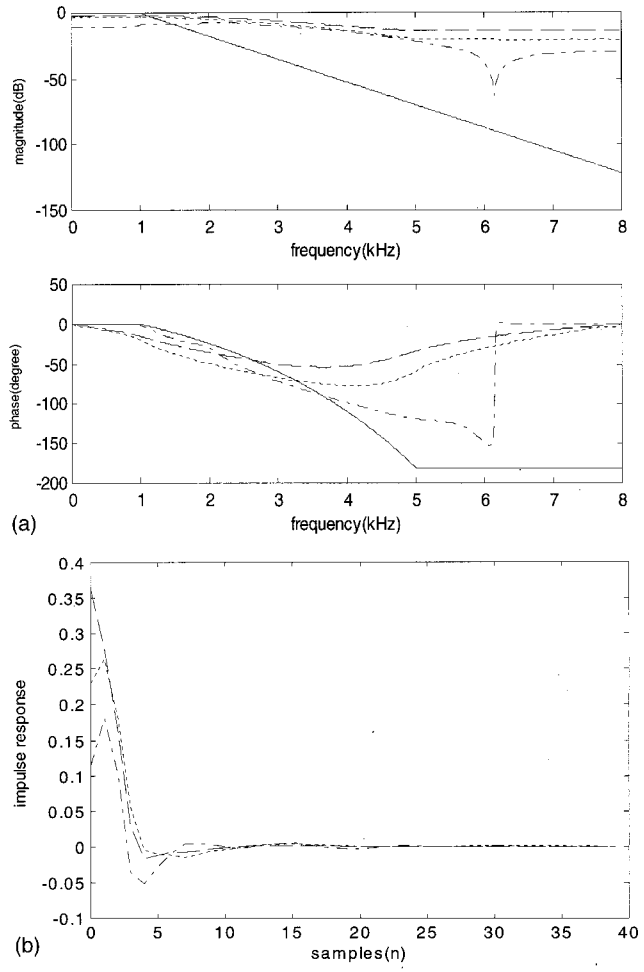


FIG. 6. Comparison of optimal filter designs using $H_1$, $H_2$, $H_\infty$ norms, respectively. (a) The frequency responses; (b) the impulse responses. template (—), 1-norm (–·–), 2-norm (···), ∞-norm (––).

duced by the filters. Instead, we selected the templates $H_d$ with minimal phase shifts within the passband. The best compromise between the stopband roll-off rate and the passband phase shift must be sought to choose the template. If there is not enough stopband roll-off, an aliasing problem will arise. On the other hand, increasing the filter roll-off will increase phase shift and degrade the performance. Once an appropriate template is chosen, it can be amended to the aforementioned optimal filter design procedure.

The model-matching criterion described in Eq. (11) is a general-purpose frequency-domain FIR filter design method. It is a simple technique that enables one to find the filter coefficients in an optimal fashion, given the frequency response specification. Different from FFT-based methods, this approach does not require the numbers of frequency samples and filter coefficients to be equal (we generally want the latter as small as possible). In this work, the frequency-domain optimization technique is employed to design both the low-pass filters required in decimation and interpolation processes, and the ANC filter $C(z)$ as well. That is, the filter template $H_d$ can be low-pass filters or $C(z)$, depending on what one is after.

An example of the optimal filter design is shown in Fig. 6. From the results, it can be observed that the $H_2$ and $H_\infty$ filters have similar trends in both frequency response and impulse response. The filter obtained from $H_1$ optimization has larger phase shift at high frequency than the other filters.

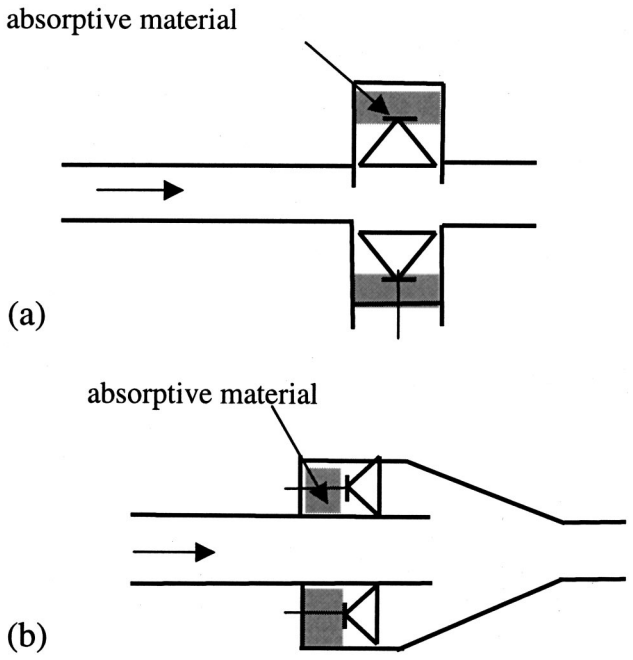


FIG. 7. Two arrangements of control loudspeaker. (a) Sideway loudspeaker; (b) backward loudspeaker.

## V. EXPERIMENTAL INVESTIGATIONS

Experiments were undertaken to compare the performance of spatially feedforward duct ANC systems with and without multirate implementation. In addition, the effects of different optimal filter designs on the control performance are also examined. A wooden duct of length 440 cm and cross section $25\times25$ cm was constructed for the experiments. If the control loudspeaker is oriented like Fig. 7(a), the controller frequency response is expressed as Eq. (3), in which an infinite number of poles will be present on the imaginary axis as a result of acoustic feedback. To mitigate the acoustic feedback, we faced the control loudspeaker towards the opening of the duct, as shown in Fig. 7(b). A practical loudspeaker differs from an ideal one-dimensional omnidirectional point source. In this configuration, Eq. (3) should be modified into

$$C' = -\frac{1}{G_{\mathrm{XDCR}}}\left(\frac{e^{-jkl_i}}{1-De^{-2jkl_i}}\right), \tag{16}$$

where $|D|<1$ signifying the ''directivity factor'' of the transducer, which is generally frequency dependent with increasing attenuation as frequency is increased. Such an approach would effectively reduce the repetitiveness of the controller impulse response (because the poles are moved away from the imaginary axis) and improve the performance as well. An extensive investigation on this technique can be found in Ref. 22. A TMS320C32 DSP equipped with four 16-bit analog IO channels is utilized to implement the controller. The sampling frequency is chosen to be 16 kHz. The up/down sampling factor is selected to be 8, rendering a nominal sampling rate of 2 kHz for the digital controller $C(z)$. Consid-

ering the cutoff frequency of the duct (approximately 700 Hz) and the poor response of the control speaker at low frequency, we chose as the control bandwidth 200 to 600 Hz. It is noted that the delays introduced by the multirate low-pass filters have been compensated by a simple ''preview'' procedure[15] in implementing $C(z)$ as follows:

(a) Measure the frequency response of the DSP in the ''echo'' mode (with only AD/DA conversions and the multirate filters), and estimate the effective delay (in samples) by $N=\Delta\Phi/360T\Delta f$, where $f$ is frequency (in Hz), $\Phi$ is the unwrapped phase (in degrees), and $T$ is the sampling period.
(b) Compensate the controller $C(z)$ by multiplying its frequency response with $\exp(j\theta N)$.
(c) Calculate the discrete-time transfer function of the compensated controller by using the MATLAB command *invfreqz*. This would effectively ''phase-lead'' compensate the controller by a phase shift $\pi f\Delta\Phi/180\Delta f$. It is also tantamount to advancing the impulse response of the controller; hence the name preview.

The active noise controller of Eq. (3) was implemented on the platform of the above-mentioned hardware system. The distance between the upstream measurement microphone and the control speaker is 2.8 m to avoid any causality problem.

In order to examine if the multirate approach is an effective method for designing low-speed digital filters in conjunction with high-speed IO channels, an experiment is conducted for comparing the conventional low sampling rate method and multirate rate method with $H_2$ optimal filter. Figure 8(a) shows the experimental results obtained from DSP implementation of both methods. Good agreement can be found in the magnitude response within the control bandwidth 200–600 Hz. However, the phase response deserves more explanation. At low sampling rate (2 kHz), the IO delay ($\delta_T$) of the conventional implementation is approximately 1.5 samples. The controller must be advanced using samples previewed by 1.5 to compensate for the delay. By multirate implementation, where the sampling rate is raised to 16 kHz, the IO delay can be reduced to only 0.7 samples (on a 2-kHz basis). The controller is then previewed by 0.7 samples to compensate for the delay. These two compensated phase responses are shown in Fig. 8(b). Good agreement can be seen in the phase response within the control bandwidth 200–600 Hz, while the discrepancy below 200 Hz could be due to the poor signal-to-noise ratio outside the band.

An experiment is then undertaken to compare various optimal filter designs used in multirate implementation (16 kHz). The result of the conventional low sampling rate implementation (2 kHz) is also included for reference. Broadband random noise is used as the primary noise. Various systems are implemented by this scenario: the first case is the conventional ANC without multirate implementation, while the next three cases are multirate ANC with $H_1$, $H_2$, $H_\infty$ optimal filters, respectively. The experimental results are shown in Fig. 8(c). Significant attenuation of noise has been obtained throughout the control bandwidth. The results are also summarized in Table III. Note that the delays introduced

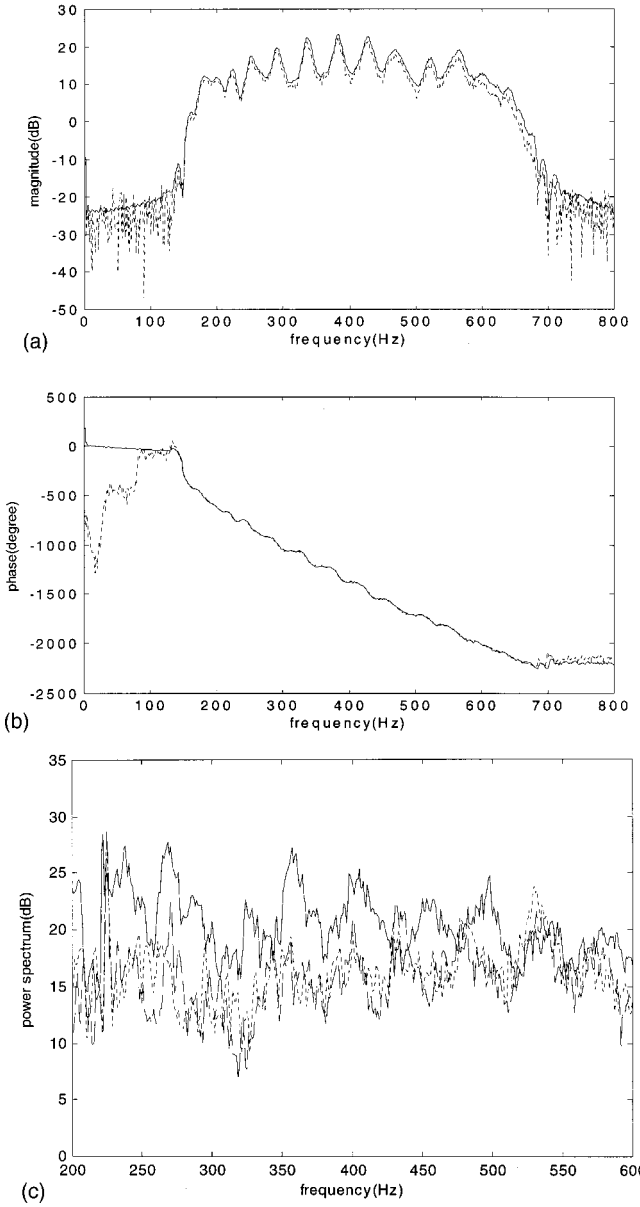


FIG. 8. The experimental results of comparison of ANC systems with and without multirate approach, using $H_2$ optimal filter. (a) The magnitude responses of controller; (b) the phase responses of controller [without multirate (———); with multirate (···)]; (c) the ANC performance [control off (—); control on, without multirate (···); control on, with multirate (––)].

by the multirate low-pass filters have been compensated by the preview procedure in implementing $C(z)$ that are optimally designed for each test case in the table. As indicated in the results, the multirate approach is able to provide better performance with less hardware complexity than the conven-

TABLE III. Summary of ANC performance for conventional and multirate implementations ($l_i=2.8$ m).

| Method | Sampling rate (kHz) | IO delay on DSP (2 kHz) (samples) | Maximum attenuation (dB) | Total attenuation (dB) |
|---|---|---|---|---|
| Conventional | 2 | 1.5 | 15.3 | 7.4 |
| Multirate $H_1$ | 16 | 0.4 | 16.8 | 6.6 |
| Multirate $H_2$ | 16 | 0.7 | 17.1 | 7.6 |
| Multirate $H_\infty$ | 16 | 0.7 | 15.2 | 7.3 |

TABLE IV. Attenuation versus distance $l_i$ for conventional and multirate implementations using $H_2$ filter. The word "ineffective" in the table refers to the case where no attenuation was observed in the experiment.

| Implementation methods | The distance $l_i$ between upstream sensor and control source (cm) | | | | | |
|---|---|---|---|---|---|---|
| | 80 | 65 | 50 | 40 | 30 | 20 |
| Conventional | 5.4 dB | 1.8 dB | ineffective | ineffective | ineffective | ineffective |
| Multirate | 6.8 dB | 6.5 dB | 6.3 dB | 5.2 dB | 2.5 dB | 1.2 dB |

tional implementation. The multirate structure based on the polyphase representation achieves not only reduction of electronic delay but also enhancement of performance of the ANC controller. In particular, the multirate ANC with $H_2$ optimal filter appears to yield the best performance (total attenuation 4.8 dB and maximum attenuation 17.3 dB). Thus, in the next experiment, we shall focus our discussion only on the multirate ANC with $H_2$ optimal filter.

At this point, one question will naturally arise. What is the limit of shortest length that one is able to achieve by using the multirate approach in the spatially feedforward duct ANC system? On the basis of the delay estimation procedure depicted in Fig. 3, the total electronic delay is estimated as 1.6 samples (with details presented in Table II). To ensure a causal controller, this in turn renders the minimal length $l_i = 23$ cm, which is a remarkable improvement owing to the considerable reduction in the analog filter delay and digital IO delay. To justify the above theoretical prediction, the experiment is repeated for $l_i = 80$, 65, 50, 40, 30, and 20 cm, respectively. The results are summarized in Table IV. Both the conventional approach and multirate approach with the $H_2$ optimal filter have produced attenuation for $l_i = 80$ and 65 cm. However, for shorter lengths the conventional method begins to lose performance, whereas the multirate method remains effective in achieving broadband attenuation, as shown in Fig. 9. The word "ineffective" in the table refers to the case where no attenuation was observed in the experiment. For brevity, only the results for $l_i = 50$ and 20 cm are shown. As expected, the performance deteriorates with decreasing length.

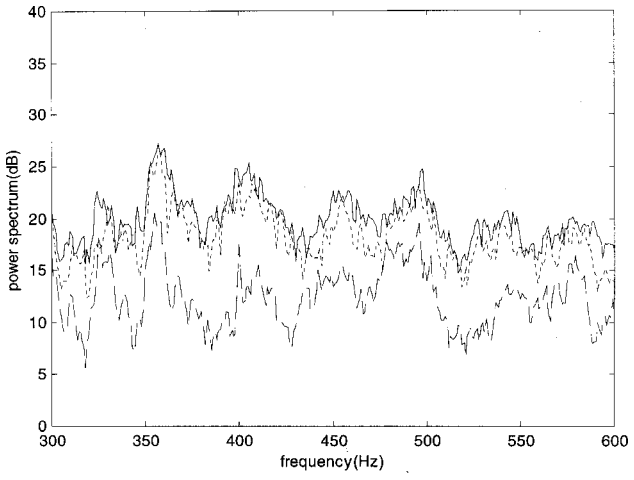


FIG. 9. The experimental results of ANC performance for $l_i = 20$ and 50 cm, using multirate implementation with $H_2$ optimal filter. control off (—), on (20 cm) (···), control on (50 cm) (––).

## VI. CONCLUSIONS

This paper suggests three potential contributions. First, this work represents the first application of a multirate ANC system to duct problems. Second, the significance of delay to the spatially feedforward system with strong acoustic feedback is thoroughly examined in the paper. Third, details of how one should implement the multirate scheme in the context of ANC applications are presented, and how effective the approach would be with regard to physical dimension is quantitatively evaluated. A detailed analysis of causality for spatially feedforward ANC systems reveals that electronic delay dictates the minimal upstream measurement microphone spacing $l_i$. A multirate approach has been developed in this work for reducing the electronic delay in the control loop. Analog low-pass filters were replaced by direct decimation and interpolation, through the use of digital filters. The computation efficiency is further enhanced by a polyphase representation, where the phases of low-pass filters must be carefully designed to avoid unnecessary delays. Frequency domain optimization procedures based on $H_1$, $H_2$, and $H_\infty$ norms, respectively, are utilized to facilitate the FIR filter design. Experimental results demonstrated the effectiveness of the multirate approach in suppressing a broadband random noise in a spatially feedforward duct ANC system. In particular, the $H_2$ design yielded the best results because it has the smallest phase shift in low-pass filtering.

However, some possibilities remain for improvement of the proposed techniques. For instance, better FIR filter design should be sought, concentrating on the vicinity of cutoff where distortions are likely to arise. The up/down sampling factor (currently 8) should be increased to further reduce the delay. The active controller was implemented as a fixed digital filter in this paper. However, in an adaptive system, this multirate technique can be highly useful. On the basis of this work, these aspects shall be explored in the future research.

## ACKNOWLEDGMENTS

The work was supported by the National Science Council in Taiwan, Republic of China, under the Project Number NSC 89-2212-E-009-007. The authors also thank the technical editor, Dr. M. Stinson, for providing the faxed copy of Ref. 14.

[1] S. J. Elliott and P. A. Nelson, "Active noise control," IEEE Signal Process. Mag. **10**, 12–35 (1993).
[2] R. F. La. Fontaine and I. C. Shepherd, "An experimental study of a broadband active attenuator for cancellation of random noise in ducts," J. Sound Vib. **91**, 351–362 (1983).
[3] M. A. Swinbanks, "The active control of sound propagation in long ducts," J. Sound Vib. **27**, 411–436 (1973).

[4] S. M. Kuo and D. R. Morgan, *Active Noise Control Systems: Algorithms and DSP Implementations* (Wiley, New York, 1995).
[5] J. C. Doyle, B. A. Francis, and A. R. Tannenbaum, *Feedback Control Theory* (Macmillan, New York, 1992).
[6] R. E. Crochiere and L. R. Rabiner, *Multirate Digital Signal Processing* (Prentice-Hall, Englewood Cliffs, NJ, 1983).
[7] P. P. Vaidyanathan, *Multirate Systems and Filter Banks* (Prentice-Hall, Englewood Cliffs, NJ, 1993).
[8] P. P. Vaidyanathan, ''Design and implementation of digital FIR filters,'' in *Handbook on Digital Signal Processing*, edited by D. F. Elliott (Academic, Cambridge, UK, 1987), pp. 55–172.
[9] M. Bellanger, G. Bonnerot, and M. Coudreuse, ''Digital filtering by polyphase network: Application to sample rate alteration and filter banks,'' IEEE Trans. Acoust., Speech, Signal Process. **ASSP-24**, 109–114 (1976).
[10] P. P. Vaidyanathan and V. C. Liu, ''Classical sampling theorems in the context of multirate and polyphase digital filter bank structures,'' IEEE Trans. Acoust., Speech, Signal Process. **ASSP-36**, 1480–1495 (1988).
[11] J. S. Arora, *Introduction to Optimum Design* (McGraw-Hill, New York, 1989).
[12] S. Boyd, L. Vandenberghe, and M. Grant, ''Efficient convex optimization for engineering design,'' in Proceedings of the IFAC Symp. Robust Contr. Design, Rio de Janeiro, Brazil, Sept. 1994.
[13] A. Grace, MATLAB *optimization toolbox* (The Mathworks, 1995).
[14] A. J. Brammer, G. J. Pan, and R. B. Crabtree, ''Adaptive feedforward active noise reduction headset for low-frequency noise,'' Proceedings ACTIVE 97 (Budapest, Hungary, August, 1997).
[15] M. R. Bai, Y. J. Lin, and J. D. Wu, ''Analysis and DSP implementation of a broadband duct ANC system using spatially feedforward structure,'' ASME J. Vibr. Acoust. **123**, 129–136 (2001).
[16] M. L. Munjal and L. J. Eriksson, ''An analytical, one-dimensional, standing-wave model of a linear active noise control system in a duct,'' J. Acoust. Soc. Am. **84**, 1086–1093 (1988).
[17] M. T. S. Tomizuka and K. K. Chew, ''Analysis and synthesis of discrete-time repetitive controllers,'' ASME J. Dyn. Syst., Meas., Control **111**, 353–358 (1989).
[18] R. H. Small, ''Closed-box loudspeaker systems. I. Analysis,'' J. Audio Eng. Soc. **20**, 798–808 (1972).
[19] P. A. Nelson and S. J. Elliott, *Active Control of Sound* (Academic, San Diego, 1992).
[20] R. A. Burdisso and C. R. Fuller, ''Causality analysis of feedforward controlled systems,'' J. Acoust. Soc. Am. **94**, 234–242 (1993).
[21] B. Noble, *Applied Linear Algebra* (Prentice-Hall, Englewood Cliffs, NJ, 1969).
[22] J. D. Wu and M. R. Bai, ''Effects of directional microphone and transducer in spatially feedforward active noise control system,'' Jpn. J. Appl. Phys. **40**, 6133–6137 (2001).